Mechanical Behavior of Fibers and Films Based on PP/Quartz Composites

E. Pérez,[1,2] C.J. Pérez,[3] C. Bernal,[4] A. Greco,[5] A. Maffezzoli[5]
[1]*National Council for Scientific and Technical Research (CONICET), Buenos Aires, Argentina*

[2]*Plastics Research and Development Center, National Institute of Industrial Technology (INTI-Plásticos), General San Martín, Buenos Aires, Argentina*

[3]*Polymer Science and Engineering Group, Materials Science and Technology Research Institute (INTEMA)-National University of Mar del Plata (UNMdP), Argentina*

[4]*Institute of Technology in Polymers and Nanotechnology, ITPN (UBA-CONICET), Engineering Faculty, University of Buenos Aires, Argentina*

[5]*Department of Engineering for Innovation, University of Salento, Monteroni, Lecce, Italy*

In this work, films and fibers of Polypropylene based composites reinforced with quartz were investigated. The materials were processed in a twin screw extruder with filler contents of 1, 2.5, and 5 wt%. Morphology, thermal properties, and mechanical behavior of these materials were studied. A homogeneous filler dispersion and particle alignment in the extrusion direction was detected for the films. Thermograms displayed a marginal nucleating effect of quartz particles. Uniaxial tensile tests indicated a high ductility level and strain hardening for the composites processed as films (in the extrusion direction). Single fiber tests displayed improved tensile properties compared with the same materials produced as films. Quasi-static fracture tests showed a completely ductile behavior for the films in the extrusion direction. In addition, films fracture toughness was found to increase with filler content. **POLYM. COMPOS., 00:000–000, 2015.** © **2015 Society of Plastics Engineers**

INTRODUCTION

Composite materials based on polymer matrices reinforced with rigid fillers have been extensively investigated in the last decades as a possible way to improve the mechanical properties of thermoplastics. In particular, the mechanical behavior finally exhibited has been related to many different parameters: components properties and content, internal structures and interactions, morphologies, processing, among others [1–8]. Different studies (morphological observations, thermal and rheological analyses, mechanical tests, and theoretical predictions) can be performed to understand the effect and relation between these factors and the mechanical properties [4, 9–15]. All of these characterizations do not easily determine the effect of each involved factor, meaning that complementary analyses should be performed.

Manufacturing techniques (method and parameters considered) can significantly affect the mechanical properties of polymer composites. Processing affects the polymer matrix characteristics (crystallinity content and morphology, drawing effect on the orientation of amorphous and crystalline phases, thermomechanical degradation, etc.) as well as the internal structure related to the presence of the reinforcing phase (filler dispersion and orientation, flaws, skin/core behavior, etc.) [12, 16–21]. Many different processing methods have been developed; some of them are extensively used due favorable performances observed. In particular, film and fiber extrusion are both associated with drawing, which affects the properties and morphology of the filled polymer [22–28]. Polymer films are often filled with inorganic particles leading to improved mechanical and barrier properties, among others. Filled polymer films are much easier produced, characterized and their mechanical behavior has been extensively studied. However, fillers in polymer fibers are rarely used, as a consequence of their effects on mechanical properties, arising from filler dispersion and the

Correspondence to: E. Pérez; e-mail: eperez@inti.gob.ar
DOI 10.1002/pc.23731
Published online in Wiley Online Library (wileyonlinelibrary.com).

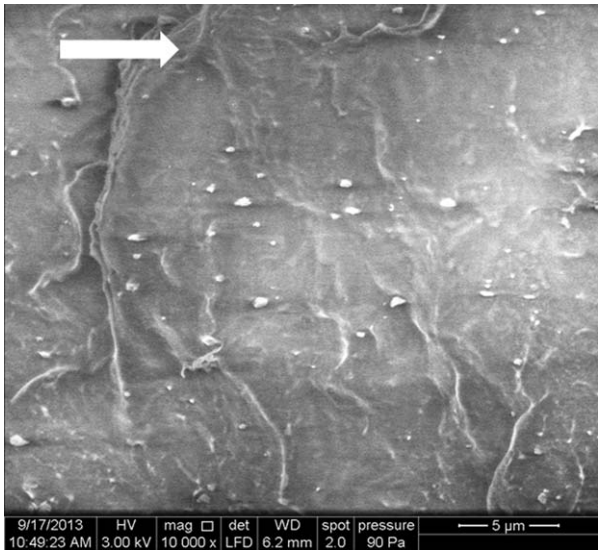

FIG. 1. Morphology of the PP-2.5 film.

related presence of defects, which can dramatically reduce their tensile properties. Therefore, both geometries deserve to be studied, since the properties of polymer

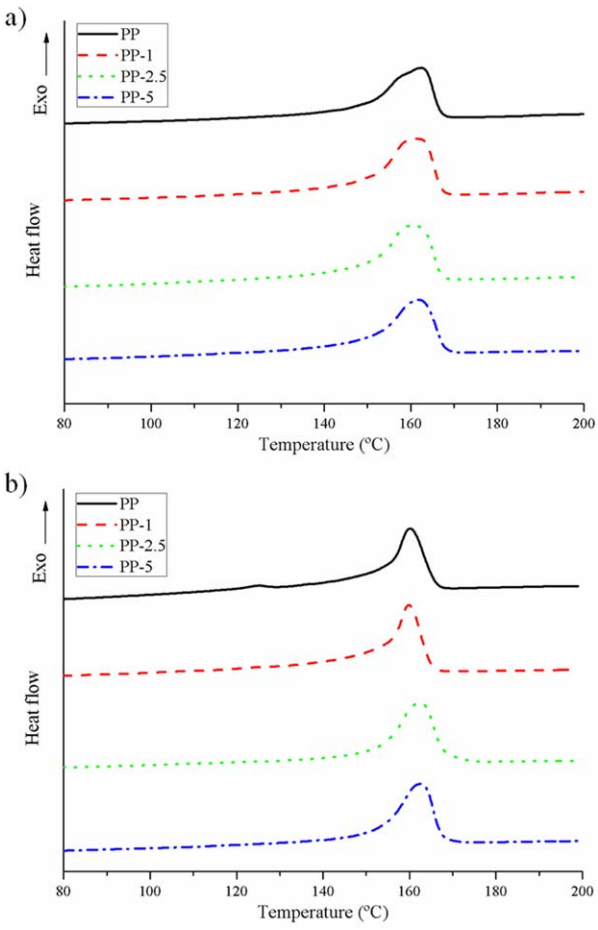

FIG. 2. DSC thermograms (first heating) of PP-quartz: (a) films and (b) fibers. [Color figure can be viewed in the online issue, which is available at wileyonlinelibrary.com.]

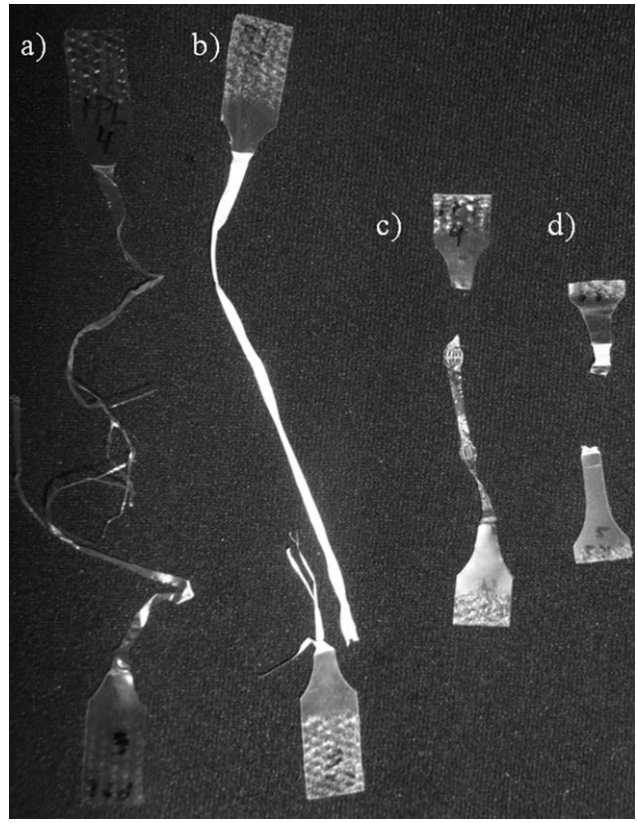

FIG. 3. Tensile samples: (a) PP, (b) PP-5 longitudinal direction, (c) PP, and (d) PP-5 transversal direction.

composite films cannot be easily repeated in composite fibers. For this reason, the gained information from the study of films can be used to better understand the fiber behavior.

In this work, Polypropylene based composites reinforced with quartz were obtained as films and fibers. Morphological observations and thermal studies were carried out. Mechanical properties were evaluated through uniaxial tensile tests and quasi-static fracture tests.

MATERIALS AND METHODS

Fibers and Films Processing

Polypropylene (melt flow index 1.8 g/10 min, CUYOLEN 1102H, Petroquímicacuyo SAIC, Argentina) and

TABLE 1. Thermal properties of PP-quartz films and fibers.

	T_c (°C)	T_f (°C)	X_c (%)
Films			
PP	116.6	162.1	42
PP-1	119.5	161.2	48
PP-2.5	120.7	160.3	48
PP-5	120.6	161.7	43
Fibers			
PP	115.7	160.1	44
PP-1	118.3	159.8	45
PP-2.5	120.1	162.3	45
PP-5	120.9	162.2	43

DOI 10.1002/pc

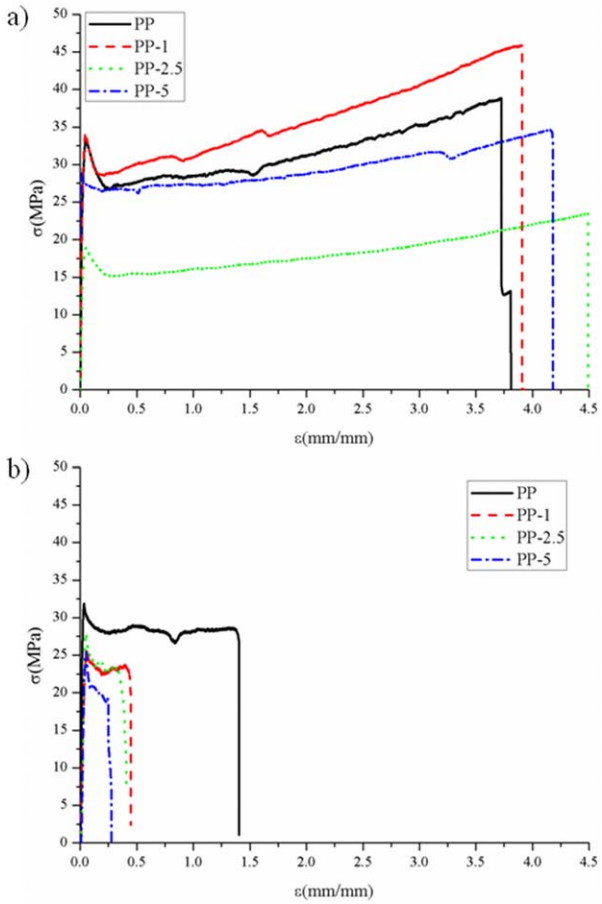

FIG. 4. Stress-strain curves for tested films in: (a) longitudinal and (b) transversal extrusion direction. [Color figure can be viewed in the online issue, which is available at wileyonlinelibrary.com.]

quartz particles (Piedra Grande, Argentina) were used as the matrix and the reinforcement of the composites, respectively. Raw quartz particles were milled in an attrition mill for 16 h. Initially, PP with 10 wt% of filler was compounded in an intensive mixer (50 r.p.m., 190°C, 10 min). The obtained blend was further mixed with neat PP in a twin screw extruder (Rheomex OS) to obtain films and fibers with: 1, 2.5, and 5 wt% of milled quartz.

Films were extruded (15 r.p.m, 215°C) and collected by a puller (Ø = 100 mm, 50 r.p.m.) obtaining a nominal thickness of 100 μm. The fibers were extruded (2 r.p.m., 200°C, die diameter = 1 mm) and collected by a winder (Ø = 12.7 mm, 100 r.p.m) obtaining a nominal diameter of 50 μm. Films and fibers were drawn in air at room temperature.

Morphological Characterization

Qualitative filler dispersion analysis was performed, for both processing methods. Cryofractured surfaces of the different materials were observed by scanning electron microscopy (SEM; FEI QUANTA 250).

Thermal Testing

Thermal analysis of films and fibers samples was performed on a Perkin Elmer Pyris 1 Differential Scanning Calorimeter (DSC) under nitrogen atmosphere at a heating rate of 10°C/min in the range of 20–200°C. Crystallinity (X_c) was determined from the DSC curves with the following expression [29]:

$$Xc(\%) = \frac{\Delta H}{(1-Ø)*\Delta H^*} * 100 \quad (1)$$

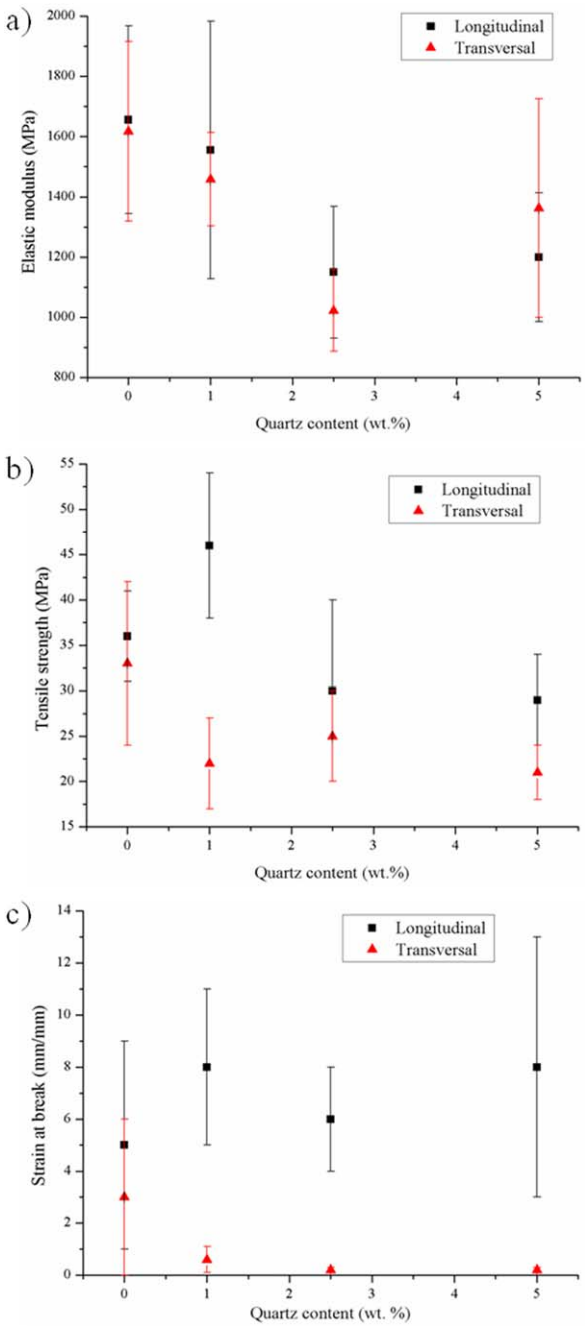

FIG. 5. Tensile parameters values for PP-quartz composite films: (a) elastic modulus, (b) tensile strength, and (c) strain at break. [Color figure can be viewed in the online issue, which is available at wileyonlinelibrary.com.]

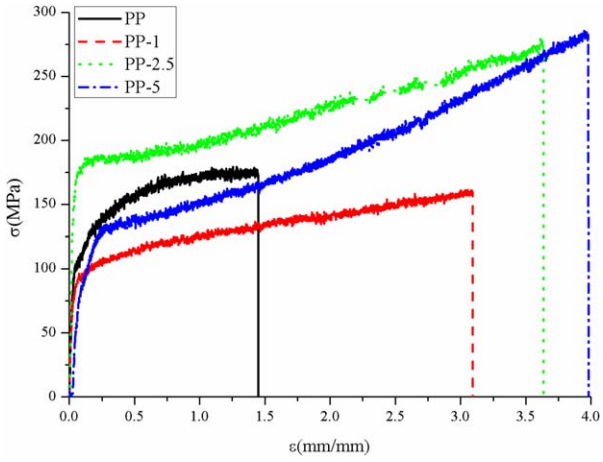

FIG. 6. Stress-strain curves for PP-quartz composite fibers. [Color figure can be viewed in the online issue, which is available at wileyonlinelibrary.com.]

where: ΔH is the measured heat of fusion, ΔH^*(209 J/g) the heat of fusion for 100% crystalline PP and Ø is the filler weight fraction [30].

Mechanical Testing

All mechanical tests were performed under quasi-static loading conditions in an INSTRON 1125 dynamometer at room temperature. Uniaxial tensile tests were performed for the films at a crosshead speed of 5 mm/min following ASTM D 638 standard recommendations. Single fiber tests were carried out at 10 mm/min in accordance with ASTM D 3379 standard recommendations. For each material and processing method a minimum of five samples were tested.

For the films, quasi-static fracture tests were performed on deeply double edge-notched (DENT) samples (length = 50 mm and width = 20 mm) at 1 mm/min with a grips distance of 30 mm. Two properly aligned sharp notches of variable length were introduced by sliding a fresh razor blade.

Fracture Toughness Characterization

The *J*-integral and Essential Work of Fracture (EWF) theories were considered to characterize the materials fracture toughness. More detailed information about these theories and their experimental procedure can be found in the literature [9, 31–33]. For each material, the applicable theory was defined based on the experimental behavior exhibited by the tested samples.

The *J*-integral approach was determined by the following expression:

$$J = \frac{\eta * U}{B * (W - a)} \tag{2}$$

where: U is the fracture energy and B, W, a are the thickness, width and notch length of the specimen, respectively. The U values were obtained by integration of the load-displacement curves up to the maximum load (J_{max} parameter) or up to the instability point (J_c parameter). These parameters were adopted to characterize materials with ductile-brittle transition or ductile instability, respectively [34]. The geometrical factor (η) for DENT samples is [32]:

$$\eta = -0.06 + 5.99\left(\frac{a}{W}\right) - 7.42\left(\frac{a}{W}\right)^2 + 3.29\left(\frac{a}{W}\right)^3 \tag{3}$$

The EWF theory considers the fracture energy (W_f) as two distinguishable terms. The specific essential work of

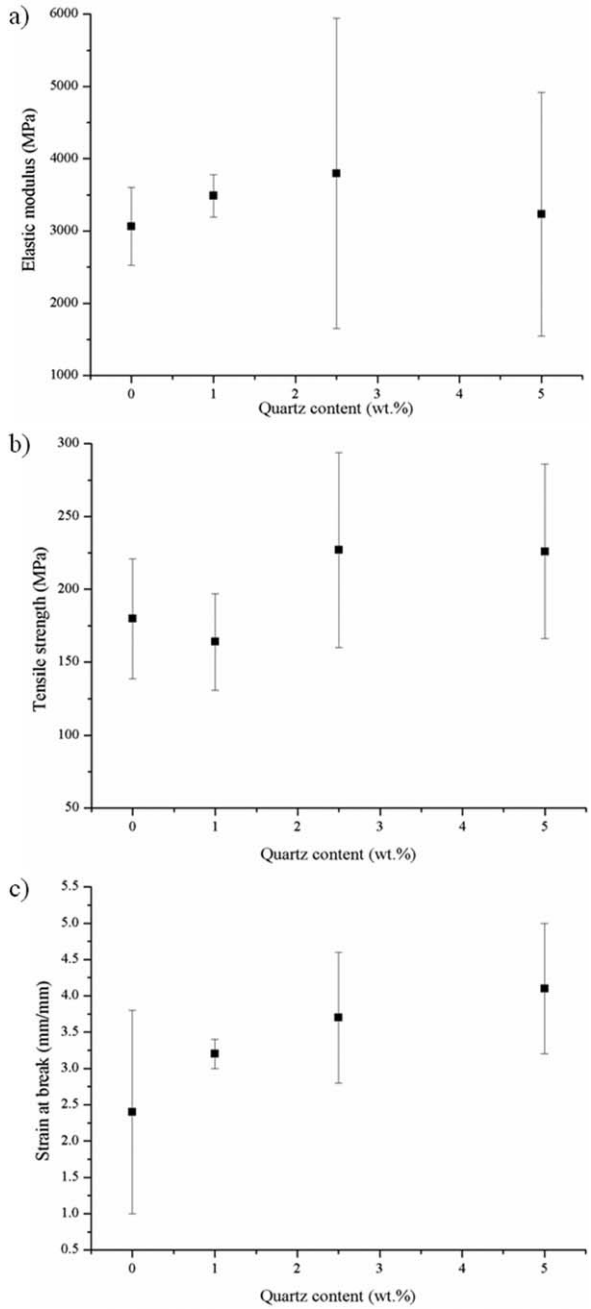

FIG. 7. Tensile parameters values for fibers: (a) elastic modulus, (b) tensile strength, and (c) strain at break.

DOI 10.1002/pc

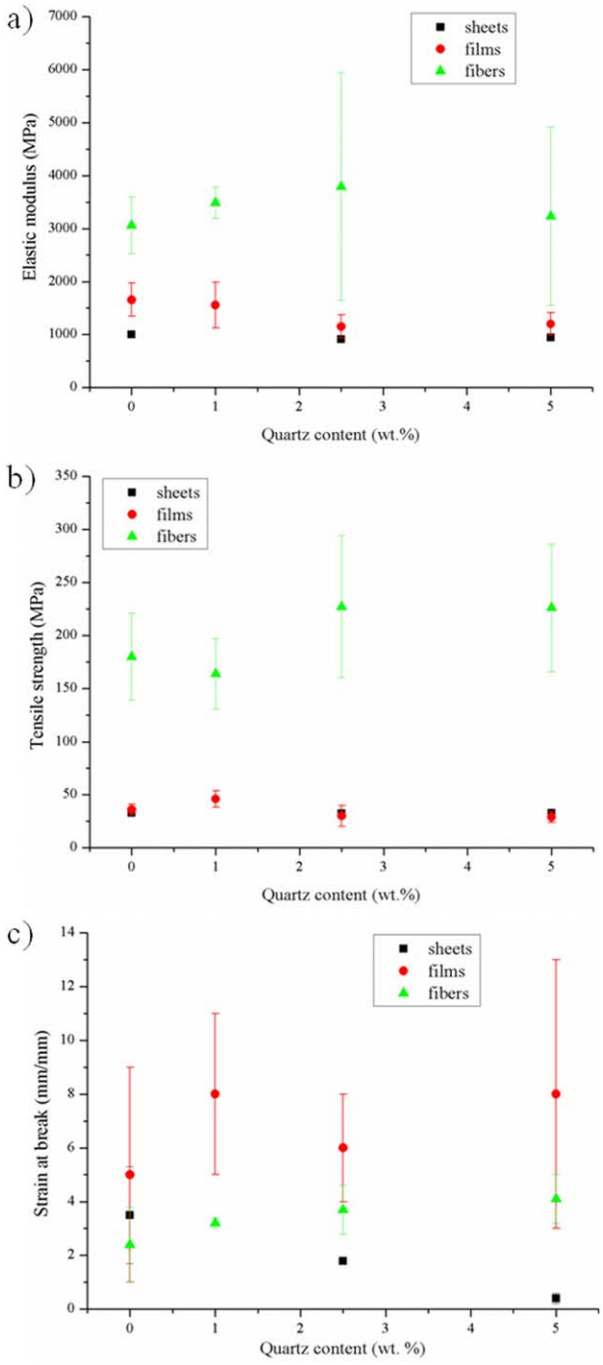

FIG. 8. Comparative tensile parameter values for PP-quartz composites: (a) elastic modulus, (b) tensile strength, and (c) strain at break. [Color figure can be viewed in the online issue, which is available at wileyonlinelibrary.com.]

fracture (w_e) related to the ligament cross section and the specific non-essential work of fracture (w_p) related to the volume placed around. The specific fracture energy (w_f) can be obtained dividing the whole energy to the ligament cross section:

$$w_f = W_f(l.t) = w_e + \beta.w_p.l \quad (4)$$

where: l is the ligament and t the specimen thickness.

The w_e and $\beta.w_p$ values can be obtained from linear regression in a diagram of specific fracture energy versus ligament length. These parameters are determined by the intercept to the w_f axis and the linear regression slope, respectively.

RESULTS AND DISCUSSION

Morphological Analysis

SEM analysis indicated that quartz particles were homogenously dispersed into the matrix for fibers and films. However, the filler (mean maximal length = 0.3 μm, mean aspect ratio = 1.4) characterized by an aspect ratio slightly >1, was aligned in the extrusion direction of films (indicated by an arrow in Fig. 1). This kind of morphology (homogeneous filler dispersion and particle alignment) is expected to be favorable for material mechanical properties in the alignment direction, as it has been reported for similar systems [22, 23, 35].

Thermal Analysis

The thermal behavior of films and fibers exhibited similar melting peak temperatures (Fig. 2a and Table 1) even though sharper peaks are observed in the case of fibers. For the films, PP matrix and composites with filler contents lower than 5 wt%, the double melting peaks suggests broader lamellar thickness. However, single and higher melting peaks evidence a more homogeneous morphology [22, 35, 36].

In general, slight increases of crystallization temperatures and crystallinity (<10%) for the composites respect to the PP matrix suggest a nucleation effect of milled quartz particles even if they are not very effective [22, 35, 37].

Mechanical Behavior

Films Uniaxial Tensile Behavior. Figure 3 shows tested samples of PP matrix and PP-5 composite films in the longitudinal and transversal extrusion direction. In the longitudinal direction, stable necking formation and stress whitening was exhibited by films samples. For the other test direction, reduced ductility was observed.

Figure 4 shows the stress-strain curves for the PP-quartz films. A high ductility level and strain hardening was displayed in the longitudinal direction (Fig. 4a), whereas reduced tensile toughness (Fig. 4b) was detected in the transversal direction. Tensile parameters values (Fig. 5) displayed different trends varying the test direction and the filler content. Elastic modulus (Fig. 5a) slightly decreased with filler content for both tested directions. The maximum tensile strength value (Fig. 5b) was detected for PP-1 in the longitudinal direction. Generally, strain at break (Fig. 5c) in transversal direction drastically decreases for composite materials with large filler

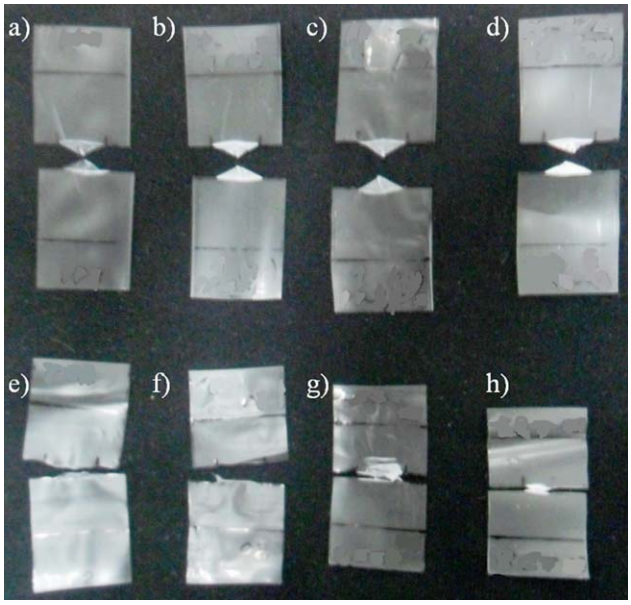

FIG. 9. Quasi-static fractured samples in the longitudinal direction: (a) PP, (b) PP-1, (c) PP-2.5, (d) PP-5, and transversal direction: (e) PP, (f) PP-1, (g) PP-2.5, and (h) PP-5. [Color figure can be viewed in the online issue, which is available at wileyonlinelibrary.com.]

contents. The extensive presence of agglomerates, flaws or discontinuities restrict the reorientation of the matrix in the tensile load direction. This effect is related to the characteristic time of deformation that is too high in comparison with that of the matrix [2, 7, 8]. In addition, in our films, no significant changes in ductility were observed in the longitudinal direction due to the matrix orientation induced by the drawing [36, 38]. The observed tensile strength and ductility trends are also related to a weak matrix/filler interaction [39].

Single Fiber Test Behavior. Tensile curves (Fig. 6) obtained in single fiber tests showed increased ductility and strain hardening with filler content, leading to an improvement of material toughness. The elastic modulus (Fig. 7a) remained roughly constant, independently of filler content. However, tensile strength (Fig. 7b) and strain to break values (Fig. 7c) increased with filler content even if a quite high scatter of experimental data is observed. It can be highlighted that similar tensile parameters values have been reported for PP fibers by other authors [40–42]. The improved mechanical performance of fibers, respect to the films, can be probably related to

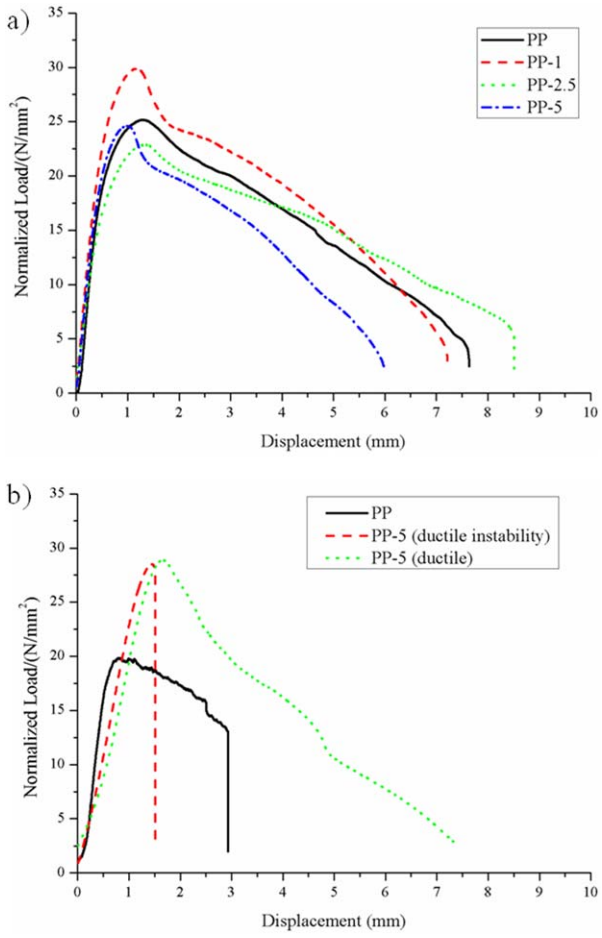

FIG. 10. Load-displacement curves for PP-quartz composite films: (a) longitudinal and (b) transversal extrusion direction. [Color figure can be viewed in the online issue, which is available at wileyonlinelibrary.com.]

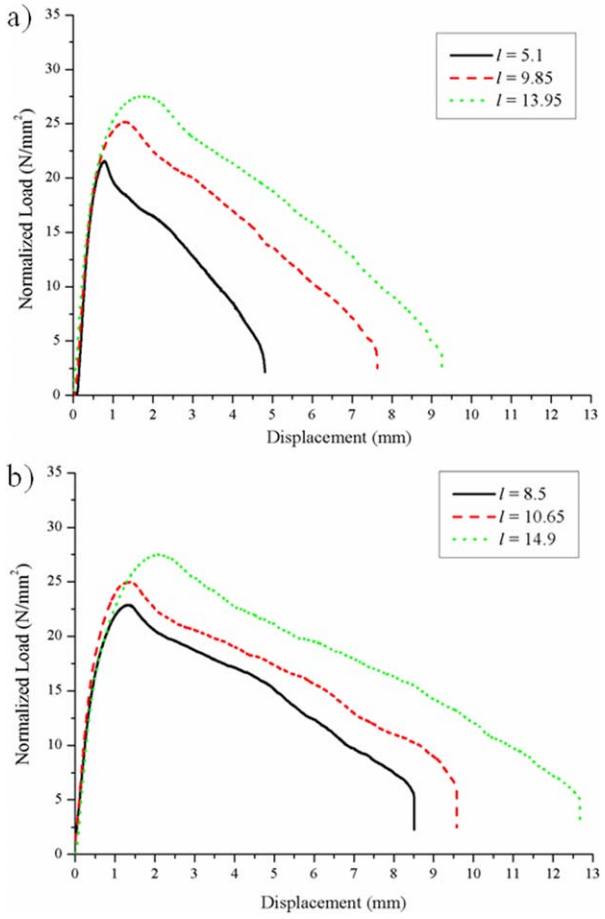

FIG. 11. Load-displacement curves for: (a) PP and (b) PP-2.5 tested in the longitudinal direction, as examples. [Color figure can be viewed in the online issue, which is available at wileyonlinelibrary.com.]

DOI 10.1002/pc

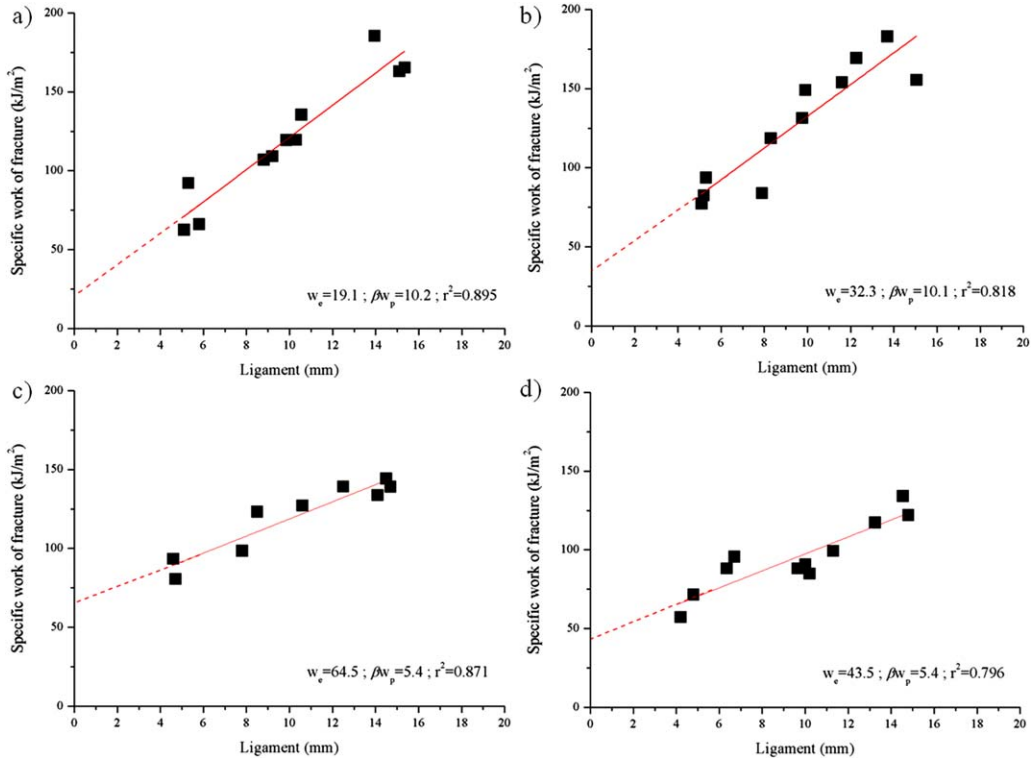

FIG. 12. EWF parameters for: (a) PP, (b) PP-1, (c) PP-2.5, and (d) PP-5 tested in the longitudinal direction. [Color figure can be viewed in the online issue, which is available at wileyonlinelibrary.com.]

a higher polymer chain and filler orientation degree due to the drawing method [22, 35, 43].

Tensile Properties Related to Processing Methods. Figure 8 compares tensile parameters values for the matrix and the PP-quartz composites processed as sheets, films (longitudinal direction) and fibers. The tensile behavior of compression molded sheets has been previously reported [44]. For the fibers, improved elastic modulus (Fig. 8a), tensile strength (Fig. 8b) and reduced strain at break values (Fig. 8c) indicate higher amorphous and crystalline orientation achieved during processing [17, 28, 45]. However, this orientation effect can be estimated to be quite low based on the high ductility level exhibited [23, 46]. The larger values of strain at break for films and fibers (Fig. 8c), compared to sheets, suggest more favorable internal morphologies (filler orientation, particle dispersion, polymer chain orientation, etc.) [22]. In addition, a specimen size effect related to lower defect frequency could simultaneously contribute to mechanical properties enhancement [35].

Quasi-static Fracture Behavior. Fracture tests were carried out on films samples cut longitudinally and transversally to the extrusion direction. For these test directions, crack propagates on the transversal and longitudinal direction, respectively. In the longitudinal extrusion direction, all materials exhibited ligament whitening and plastic deformation (Fig. 9a–d) related to ductile fracture processes. For the transversal direction (Fig. 9e–h), the PP matrix samples indicated ductile instability while for the composites the ductile-brittle transition was observed (some samples displayed ductile instability (Fig. 9e and f) whereas other samples presented completely ductile fracture (Fig. 9g and h).

Figure 10 shows load-displacement curves for samples with a notch depth/width ratio of 0.5. Load curves were normalized against sample cross-section for the sake of clarity. These curves displayed different fracture behavior in accordance with the specimen morphologies described above. For a qualitatively classification, the ductility level was considered (D_l = displacement at break/ligament) [33]. The obtained values ($1 < D_l < 1.5$) for materials tested in the longitudinal direction suggested the applicability of EWF theory. Figure 11 shows curves for the PP matrix and PP-2.5, as examples. The requirement of self-similarity for samples with variable ligament was satisfied for each analyzed material (not shown here). Fracture parameters values are plotted in Figures 12 and 13. The highest w_e value corresponded to the composite PP-2.5 while a decreasing trend of $\beta.w_p$ values with filler content was observed (Fig. 13a).

However, for transversal direction, the Jc was adopted to characterize the PP matrix toughness ($J_c = 113 \pm 46$ kJ/m^2). The J_{max} parameter values determined for the composites (Fig. 13b) did not show a clear trend with filler content.

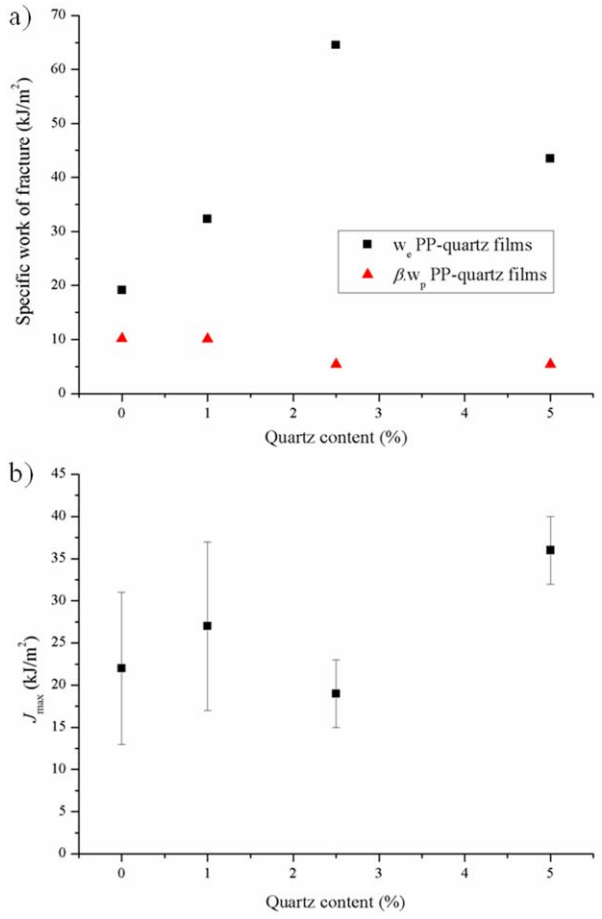

FIG. 13. Fracture parameters for films: (a) longitudinal (EWF theory) and (b) transversal direction (J_{max} parameter). [Color figure can be viewed in the online issue, which is available at wileyonlinelibrary.com.]

CONCLUSIONS

In this work, PP-quartz composites were extruded as films and fibers. The morphology, thermal and mechanical behavior were studied. The obtained results and the discussion detailed above allow obtaining the following conclusions:

- The incorporation of quartz particles led to enhancements of tensile and fracture toughness in the drawing direction, especially at low filler content.
- The extrusion process favored the composite mechanical performance, compared to compression molding, related to favorable internal structures (polymer chain and/or filler orientation, particle dispersion, low frequency internal defects, etc.).
- The fibers exhibited increased tensile parameter values. Polymer drawing can be estimated quite low but adequate to enhance the mechanical properties of PP based composites.

REFERENCES

1. C.E. Corcione, A. Cavallo, E. Pesce, A. Greco, and A. Maffezzoli, *Polym. Eng. Sci.*, **51**(4), 1280 (2001).
2. B. Cotterell, J.Y.H. Chia, and K. Hbaieb K, *Eng. Frac. Mech.*, **74**, 1054 (2007).
3. E. Fekete, J. Móczó, and B. Pukánszky, *J. Coll. Int. Sci.*, **269**, 143 (2004).
4. S.-Y. Fu, X.-Q. Feng, B. Lauke, and Y.-W. Mai, *Compos. B*, **39**, 933 (2008).
5. A. Greco, A. Maffezzoli, G. Casciaro, and F. Caretto, *Compos. B*, **67**, 233 (2014).
6. F. Hussain, M. Hojjati, M. Okamoto, and R.E. Gorga, *J. Comp. Mater.*, **40**, 1511 (2006).
7. J. Móczó, and B. Pukánszky, *J. Ind. Eng. Chem.*, **14**, 535 (2008).
8. L. Sun, R.F. Gibson, F. Gordaninejad, and J. Suhr, *Compos. Sci. Technol.*, **69**, 2392 (2009).
9. T. Bárány, T. Czigány, and J. Karger-Kocsis, *Prog. Polym. Sci.*, **35**, 1257 (2010).
10. A. Kiss, E. Fekete, and B. Pukánszky, *Compos. Sci. Technol.*, **67**, 1574 (2007).
11. B. Lauke, *Compos. Sci. Technol.*, **86**, 135 (2013).
12. T. Sun, F. Chen, X. Dong, and C.C. Han, *Polymer*, **49**, 2717 (2008).
13. C.J.R. Verbeek, *Mater. Lett.*, **57**, 1919 (2003).
14. J.G. Williams, *Compos. Sci. Technol.*, **70**, 885 (2010).
15. X.-L. Xie, Q.-X. Liu, R.K.-Y. Li, X.-P. Zhou, Q.-X. Zhang, Z.-Z. Yu, and Y.-W. Mai, *Polymer*, **45**, 6665 (2004).
16. Á. Ábrányi, L. Százdi, B. Pukánszky Jr., G.J. Vancsó, and B. Pukánszky, *Macromol. Rapid. Commun.*, **27**, 132 (2006).
17. T. Amornsakchai, R.H. Olley, D.C. Bassett, M.O.M. Al-Hussein, A.P. Unwin, and I.M. Ward, *Polymer*, **41**, 8291 (2000).
18. T. Amornsakchai and P. Songtipya, *Polymer*, **43**, 4231 (2002).
19. P. Colomban, J.M. Herrera Ramirez, R. Paquin, A. Marcellan, and A. Bunsell, *Eng. Frac. Mech.*, **73**, 2463 (2006).
20. S. Díez-Gutiérrez, M.A. Rodríguez-Pérez, J.A. De Saja, and J.I. Velasco, *Polymer*, **40**, 5345 (1999).
21. R.J. Young and S.J. Eichhorn, *Polymer*, **48**, 2 (2007).
22. M.D´ Amato, A. Dorigato, L. Fambri, and A. Pegoretti, *eXPRESS Polym. Lett.*, **6**(12), 954 (2012).
23. F.P. La Mantia, N.T. Dintcheva, R. Scaffaro, and R. Marino, *Macromol. Mater. Eng.*, **293**, 83 (2008).
24. B. Pukánszky, *Eur. Polym. J.*, **41**, 645 (2005).
25. A. Galeski, *Prog. Polym. Sci.*, **28**, 1643 (2003).
26. Y. Wang, Y. Qin, Y. Zhang, M. Yuan, H. Li, and M. Yuan, *Int. J. Biol. Macromol.*, **67**, 58 (2014).
27. X.M. Zhang and A. Ajji, *Polymer*, **46**, 3385 (2005).
28. H. Deng, C.T. Reynolds, N.O. Cabrera, N.-M. Barkoula, B. Alcock, and T. Peijs, *Compos. B*, **41**, 268 (2010).
29. W.Y. Yam, J. Ismail, H.W. Kammer, H. Schmidt, and C. Kummer-löwe, *Polymer*, **40**, 5545 (1999).
30. R.P. Quirk and M.A. Alsamire, *Polymer Handbook*, J. Branbrup and E.H. Immergut, Eds., Wiley, New York (1990).

DOI 10.1002/pc

31. ASTM International, *ASTM E 1820: Standard Test Method for Measurement of Fracture Toughness*, American Society for Testing and Materials, West Conshohocken (2001).
32. L.A. Fasce, V. Costamagna, V. Pettarin, M. Strumia, and P.M. Frontini, *eXPRESS Polym. Lett*., **2**(11), 779 (2008).
33. A.B. Martínez, J. Gamez-Pérez, M. Sanchez-Soto, J.I. Velasco, O.O. Santana, and M. Ll Maspoch, *Eng. Fail. Anal*., **16**, 2604 (2009).
34. L.A. Fasce, P.M. Frontini, S.-C. Wong, Y.-W. Mai, *J. Polym. Sci.: Part B. Polym. Phys*., **42**, 1075 (2004).
35. S. Chantrasakul and T. Amornsakchai, *Polym. Eng. Sci*., **47**, 943 (2007).
36. H. Zhao and R.K.Y. Li, *J. Polym. Sci.: Part B Polym. Phys*., **43**, 3652 (2005).
37. A. Tidjani, O. Wald, M.-M. Pohl, M.P. Hentschel, and B. Schartel, *Polym. Degrad. Stab*., **82**, 133 (2003).
38. W.C.J. Zuiderduin, C. Westzaan, J. Huétink, and R.J. Gaymans, *Polymer*, **44**, 261 (2003).
39. Y.S. Thio, A.S. Argon, and R.E. Cohen, *Polymer*, **45**, 3139 (2004).
40. M. Jose, D. Dean, J. Tyner, G. Price and E. Nyairo, *J. Appl. Polym. Sci*., **103**, 3844 (2007).
41. S. Kumar, H. Doshi, M. Srinivasarao, J.O. Park, and D.A. Schiraldi, *Polymer*, **43**, 1701 (2002).
42. N. Wanasekara, V. Chalivendra, and P. Calver, *Polym. Degrad. Stab*., **96**, 432 (2011).
43. G. Colombe, S. Gree, O. Lhost, M. Dupire, M. Rosenthal, and D.A. Ivanov, *Polymer*, **52**, 5630 (2011).
44. E. Pérez, *Development of composite materials based on Polypropylene reinforced with rigid particles*, University of Buenos Aires, Buenos Aires (2014).
45. S. Ruan, P. Gao, and T.X. Yu, *Polymer*, **47**, 1604 (2006).
46. S. Chand, G.S. Bhat, J.E. Spruiell, and S. Malkan, *Thermochim. Acta*, **367**, 155 (2001).